AR-009-804

DSTO-TR-0398

Microwave Nondestructive
Evaluation of Disbonds
Under Anechoic Tiles

R.J. Ditchburn, A.Amiet
and S.K. Burke

19970307 048

DEPARTMENT◆OF DEFENCE

DEFENCE SCIENCE AND TECHNOLOGY ORGANISATION

Microwave Nondestructive Evaluation of Disbonds Under Anechoic Tiles

R.J. Ditchburn, A.Amiet and S.K. Burke

Ship Structures and Materials Division
Aeronautical and Maritime Research Laboratory

DSTO-TR-0398

ABSTRACT

An experimental and theoretical study of a microwave nondestructive inspection technique to detect the presence of and evaluate the thickness of disbonds between anechoic tiles and the hull of the COLLINS-class submarine is presented. The magnitude and phase of a reflected microwave signal in the absence and presence of a disbond is measured as a function of disbond thickness and frequency for (i) a layer of anechoic tile material and (ii) a COLLINS anechoic tile, both backed by a flat conducting plate. Disbond thicknesses of 0.0 to 1.5 mm are considered over a frequency range of 2 to 18 GHz. The results are in good agreement with theoretical predictions and clearly indicate that disbonds of 0.1 mm can be easily detected. Further development and potential problems are also described.

RELEASE LIMITATION

Approved for public release

DEPARTMENT OF DEFENCE
◆
DEFENCE SCIENCE AND TECHNOLOGY ORGANISATION

APPROVED FOR PUBLIC RELEASE

# Microwave Nondestructive Evaluation of Disbonds Under Anechoic Tiles

Executive Summary

Anechoic tiles are adhesively bonded to the outer surface of the hull of the COLLINS-class submarines to absorb sonar signals. Concern has been raised that corrosion under these synthetic rubber tiles may proceed undetected and that the tiles may become detached during service. The RAN has requested SSMD to develop a nondestructive method for detecting disbonds and corrosion under the tiles. This is particularly difficult because the tiles are thick and attenuating and for practical reasons inspection is limited to the outside of the submarine.

This report presents an experimental and theoretical study of a candidate nondestructive inspection technique capable of detecting the presence of and measuring the thickness of disbonds between anechoic tiles and the hull of the COLLINS-class submarines. In the laboratory, a non-contact microwave technique that relies on the measurement of the magnitude and phase of a reflected microwave signal has been investigated. The magnitude and phase of a reflected microwave signal in the absence and presence of a disbond is measured for different disbond thicknesses over a range of frequencies.

A theoretical model for predicting the magnitude and phase of the reflected microwave signal in the absence and presence of a disbond has been derived. The theoretical phase calculations were in excellent agreement with experiment. The experimental results clearly indicate that disbond gaps of 0.1 mm can easily be resolved under laboratory conditions. However, further refinements are required before this technique can be implemented as a practical and reliable method for detecting disbonds under COLLINS anechoic tiles in field conditions.

Authors
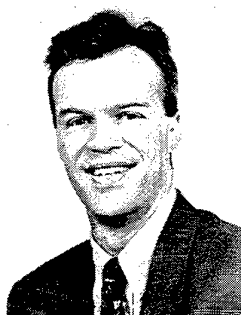
R.J. Ditchburn
Ship Structures and Materials Division

Dr Robert Ditchburn is a Research Scientist in the Ship Structures and Materials Division at AMRL. He received a B.App.Sc. (Hons) in applied physics and a Ph.D. from the University of Technology, Sydney. In 1993 Dr Ditchburn joined DSTO and has been involved in research into nondestructive testing techniques for through-life support for the COLLINS-class submarines.

A. Amiet
Ship Structures and Materials Division

Andrew Amiet is Professional Officer in the Ship Structures and Materials Division at AMRL. He received a B.Sc. (Hons) in physics from Monash University in Melbourne. He joined AMRL in 1990 and has worked in the design, production and testing of radar absorbing materials for aircraft and marine applications.

S.K. Burke
Ship Structures and Materials Division

Dr Stephen Burke is a Principal Research Scientist in the Ships Structures and Materials Division at AMRL, Fishermens Bend. He received a B.Sc. (Hons) in physics from Monash University and Ph.D. from Imperial College, London. Since joining DSTO in 1983, Dr Burke has been involved in the development of electromagnetic NDE techniques for through-life support of military aircraft, navy ships and submarines.

Contents

1. Introduction

Anechoic tiles are adhesively bonded to the outer surface of the hull of the COLLINS-class submarines to absorb sonar signals. Concern has been raised that corrosion under these synthetic rubber tiles may proceed undetected and that the tiles may become detached during service. It is therefore desirable to develop a nondestructive technique for detecting and sizing disbonds between the tiles and the hull. Many other applications involving adhesively bonded dielectric layers also occur in the construction, naval and aerospace industries where a disbond, delamination, or absence of adhesive between any two layers can lead to a major failure. Early detection of these defects is important. Often the layers are backed by a metal plate which limits inspection access to one side of the structure. This is the case for the COLLINS, and detection is further complicated by the large thickness and highly absorbing nature of the anechoic tiles.

Here we consider a nondestructive and non-contact technique not only capable of detecting the presence of a disbond between a dielectric layer and a conducting plate but also measuring the disbond thickness. The technique involves measuring the phase of a microwave signal reflected from the layered structure. Microwaves are well suited to this task, due to: (i) their ability to penetrate zero-loss and low-loss dielectric media, (ii) their high sensitivity to the presence of the boundary between two dissimilar layers, and (iii) their coherent nature, which can be used to detect phase variations as signals pass through a dielectric layer.

Zoughi and Lujan have used two methods to measure the thickness of dielectric layers in both the presence and absence of a conducting backing plate [1]. The first method involves the comparison of the amplitude of reflected signals from the boundary layers, while the second technique relies on the measurement of a phase difference between the phase of a microwave signal reflected (or transmitted) by the layered structure compared with that of a reflected reference signal. Edwards and Zoughi have extended the latter method to include a disbond layer between the dielectric layer and the conducting plate [2].

In this report the suitability of such microwave phase measurements for detecting and sizing disbonds beneath the COLLINS anechoic tiles is examined. In section 2 of this report, following Edwards and Zoughi [2], we derive an expression for the phase of the effective amplitude reflection coefficient due to a disbond between a dielectric layer and a conducting plate. This expression is verified against experiment in Section 4 using the experimental configuration described in Section 3. The sensitivity of the technique to disbond thickness is also considered in Section 4 and the optimum inspection parameters are determined. Finally , the suitability of the technique for inspection of the COLLINS anechoic tiles is discussed in Section 5, and areas for future development and potential problems are described.

2. Theoretical Formulation

The geometry of the multi-layer problem is illustrated schematically in Figure 1, where the reflection of uniform plane electromagnetic waves from two dielectric layers backed by a conducting plate has been shown. The multi-layer structure consists of a semi-infinite region of free-space, a dielectric layer and a small dielectric layer of disbond all backed by a flat conducting plate. For the purpose of this investigation each layer is assumed to be non-magnetic, isotropic and homogeneous. A dielectric material has a complex relative dielectric permittivity of $\varepsilon_r = \varepsilon'_r - j\varepsilon''_r$, where $j = \sqrt{-1}$. The real part of the relative permittivity, ε'_r, is a measure of the extent to which the material will be polarized on application of an applied external electric field and is the primary cause of signal phase variation. The imaginary part, called the loss factor, ε''_r, is a measure of the energy loss incurred in re-arranging the alignment of the electric dipoles with that electric field and is the primary cause of signal attenuation. Collectively, ε'_r and ε''_r are known as the relative dielectric constants. For a low-loss dielectric material ε''_r is much smaller than ε'_r and for a zero-loss material $\varepsilon''_r = 0$. In Figure 1, the complex relative permittivity of free-space is $\varepsilon'_0 = 1 - j0$ while the conducting plate is assumed to be a non-magnetic perfect conductor, i.e., $\varepsilon'_3 \equiv -j\infty$. The dielectric layer has a complex permittivity of ε'_1 and a thickness of d_1, whilst ε'_2 and d_2 characterize the disbond layer. If the disbond consists entirely of an air-gap, layer 2 will have $\varepsilon'_2 = 1 - j0$ and d_2 will be unknown.
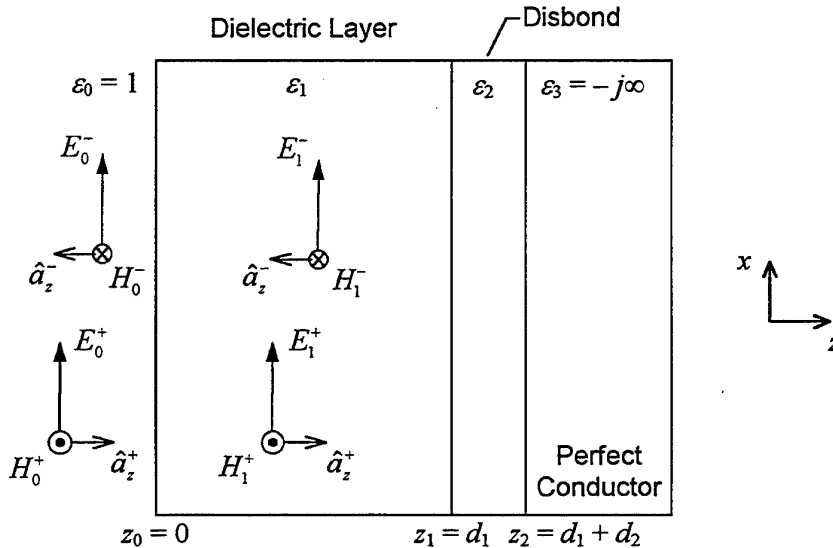

Figure 1: *Incident and reflected fields impinging on a dielectric layered structure consisting of a single dielectric layer, a disbond layer, backed by a conducting plate.*

Figure 1 shows an electric field, E_0^+, impinging the layered structure at normal incidence. E_0^+ is a uniform plane wave polarized in the x-direction and propagating in the positive z-direction. Once E_0^+ is reflected by each layer in the structure, it is detected as E_0^- which incorporates all the multiple reflections. The effective amplitude reflection coefficient (Γ) of the multi-layer structure is given by the ratio E_0^-/E_0^+. The phase difference between the effective amplitude reflection coefficient for the structure with a disbond present and one without a disbond is related to the thickness (d_2) and permittivity (ε_2^r) of the gap. If the phase difference and ε_2^r are known then d_2 can be calculated.

The electromagnetic fields in each layer can be expressed in phasor notation as

$$E_n = \hat{a}_x \left(E_n^+ e^{-j\gamma_n z} + E_n^- e^{j\gamma_n z} \right), \tag{1}$$

$$H_n = \hat{a}_y \frac{1}{\eta_n} \left(E_n^+ e^{-j\gamma_n z} - E_n^- e^{j\gamma_n z} \right), \tag{2}$$

where the + and − superscripts represent the forward (positive z-going) the backward (negative z-going) travelling waves respectively and the subscript n denotes the layer number. In the present case $n = 0, 1, 2$. Unit vectors in the x and y directions are denoted by $\hat{a}_x$ and $\hat{a}_y$ respectively. A time dependence of the form $e^{j\omega t}$ is assumed but not shown explicitly. In Equations 1 and 2 the $E_n^\pm$ fields are unknowns and can be determined by the application of the appropriate boundary conditions as described below.

In each layer, the phase propagation factor is

$$\gamma_n = k_0 \sqrt{\varepsilon_n^r}, \tag{3}$$

where ε_n^r is the relative complex permittivity of each layer and k_0 is the free-space wave number, and is given by

$$k_0 = \frac{2\pi}{\lambda_0}, \tag{4}$$

where λ_0 is the wavelength in free space. The intrinsic impedance of each layer is

$$\eta_n = \sqrt{\frac{\mu_o \mu_n^r}{\varepsilon_o \varepsilon_n^r}}, \tag{5}$$

where μ_n^r is the complex relative permeability of each layer and μ_o and ε_o are the permeability and permittivity of free-space respectively. Here $\mu_n^r = 1$, since we are considering non-magnetic layers.

The boundary conditions at z_2 are that on the surface of a perfect conductor the tangential component of the E-fields is zero, i.e., $E_2(d_1 + d_2) = 0$, giving

$$E_2^- = -E_2^+ e^{-j2\gamma_2(d_1+d_2)}. \tag{6}$$

The boundary conditions at z_o and z_1 require the tangential components of the E- and H-fields to be continuous across each boundary, resulting in

$$E_0^+ + E_0^- = E_1^+ + E_1^-, \tag{7}$$

$$\left(E_0^+ - E_0^-\right)/\eta_0 = \left(E_1^+ - E_1^-\right)/\eta_1, \tag{8}$$

$$E_1^+ e^{-j\beta_1 d_1} + E_1^- e^{j\beta_1 d_1} = E_2^+ e^{-j\beta_2 d_1} + E_2^- e^{j\beta_2 d_1}, \tag{9}$$

$$\left(E_1^+ e^{-j\beta_1 d_1} - E_1^- e^{j\beta_1 d_1}\right)/\eta_1 = \left(E_2^+ e^{-j\beta_2 d_1} - E_2^- e^{j\beta_2 d_1}\right)/\eta_2, \tag{10}$$

Solving Equations 7–10 gives the complex effective amplitude reflection coefficient, Γ, and its phase, ϕ,

$$\Gamma = \frac{E_0^-}{E_0^+} = \frac{\eta_1 C - \eta_0}{\eta_1 C + \eta_0}, \tag{11}$$

$$\phi = \tan^{-1}\left[\frac{\text{Im}(\Gamma)}{\text{Re}(\Gamma)}\right], \tag{12}$$

where

$$C = \frac{1 + B e^{-j2\gamma_1 d_1}}{1 - B e^{-j2\gamma_1 d_1}}, \tag{13}$$

$$B = \frac{\eta_2 A - \eta_1}{\eta_2 A + \eta_1}, \tag{14}$$

$$A = \frac{1 - e^{-j2\gamma_2 d_2}}{1 + e^{-j2\gamma_2 d_2}}. \tag{15}$$

4

The reflectance (or intensity reflection coefficient), R, which is a measurable quantity, can be determined from Equation 11, giving

$$R = |\Gamma|^2. \tag{16}$$

Finally, if the phase is to be measured by normalizing with respect to the perfectly conducting substrate (Fig. 2), the normalized phase is given by

$$\phi_{normalized} = \phi - \phi_{perfect\,conductor}. \tag{17}$$

It should be noted that in Equation 17, z_2 is the same for both ϕ and $\phi_{perfect\,conductor}$ to ensure that the phases are being calculated at the same distance from the surface of the perfect conductor. In practice an exposed region of the conducting substrate could be used. Alternatively, as was done by Zoughi and Lujan [1], a thin conducting foil placed in contact with the front of the dielectric structure can be used to measure the reference phase. In what follows we reference all phase measurements to the top surface of the conducting substrate, and all phase measurements refer to the normalized case unless specifically stated. For simplicity the subscript normalized has been dropped.

In our approach the problem has been confined to a single dielectric layer and one disbond layer, however this technique is equally valid for any number of dielectric layers. Equations for two dielectric layers and a single disbond are given in references [3] and [4].
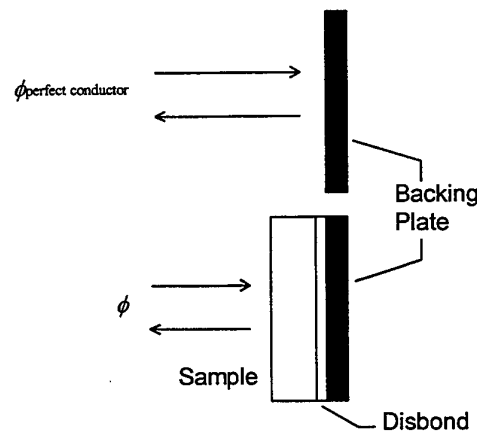

Figure 2: Schematic diagram showing the two phase measurements needed to calculate the normalized phase.

3. Experimental

3.1 Reflectance Measurements

The experimental set-up is shown in Figure 3. The phase and reflectance were measured using a Hewlett-Packard 8510B vector network analyser, in conjunction with an HP8350B Sweep Oscillator, an HP83592A RF Plug-in and an HP8512 Reflection/Transmission test set. The system is capable of measuring magnitude and phase between 500 MHz and 18 GHz. The near-normal incidence ($\theta = 3°$) phase and reflectance measurements were made using a dual horn technique with separate send and receive horn antennae over the frequency range of 2 to 18 GHz. Time gating was applied to the measured signal to reduce unwanted reflections from the test area.

The theoretical derivation in Section 2 assumes that all fields in the layers are uniform plane electromagnetic waves so that it is essential that the dielectric structure to be measured is placed in the far-field of the microwave horns. The sample size was set to ensure far-field conditions were satisfied, i.e., less than a $\pi/8$ phase difference from the centre to the edge of the sample at 18 GHz. The sample size was 150 mm square while the distance between the horns and the sample was 3 m.

The reflected phase was calibrated with respect to a conducting aluminium plate. These measurements were subtracted from subsequent phase measurements to obtain the normalized phase. A homogeneous isotropic synthetic rubber dielectric layer was placed in intimate contact with the front of the aluminium plate, representing the case of no disbond. Individual sheets of paper placed between the aluminium plate and dielectric layer were then used to achieve small uniform disbond layers. Each 150 mm square sheet of paper has a thickness of 0.1 mm and a measured permittivity of $\varepsilon_r = 4$. Disbond thicknesses ranging 0 to 1.5 mm were investigated over the frequency range 2 to 18 GHz, which corresponds to wavelengths, λ_0, from 149.9 to 16.7 mm respectively. This procedure was repeated using a COLLINS anechoic tile in place of the isotropic dielectric layer.
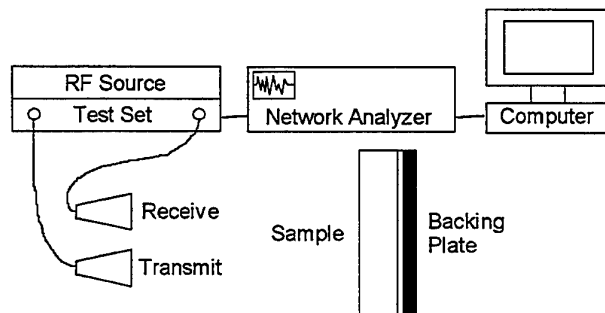

Figure 3: Schematic diagram showing the experimental apparatus used for the phase measurement.

3.2 Permittivity Measurements

The permittivity of the paper and the low-loss isotropic synthetic rubber layer were measured using a transmission method developed at AMRL. Two horn antennae were placed on opposite sides of the sample at distance apart of approximately 500 mm. The magnitude and phase of the transmitted signal was measured from 7.5 to 18 GHz and the complex permittivity of the sample determined, assuming the magnetic permeability of the sample is identical to that of free space. This assumption is valid since there are no magnetic inclusions in the sample.

4. Results

Experiments were performed on two different samples; (i) a homogeneous isotropic synthetic rubber layer composed of anechoic tile material and (ii) a COLLINS anechoic tile. In Section 4.1 the experimental results for the isotropic layer are presented and compared with theoretical results while in Section 4.2 the experimental results for the anechoic tile are presented. For both samples the sensitivity to disbond thickness is shown and the optimum inspection parameters are determined.

4.1 Isotropic Synthetic Rubber Layer

The complex relative dielectric permittivity of the low-loss isotropic synthetic rubber layer and paper were measured by the method described in Section 3.2. The synthetic rubber is characterized by $\varepsilon_1^r = 15.0 - j0.7$ and $d_1 = 24.4$ mm. For modelling purposes $\varepsilon_0^r = 1 - j0$ and $\varepsilon_3^r \equiv -j\infty$. The disbond properties are given by the measured permittivity of paper, $\varepsilon_2^r = 4 - j0$ and $d_2 =$ thickness of paper sheet(s). All theoretical calculations were carried out assuming normal incidence.

The theoretically calculated phase of a reflected wave from a perfect conductor ($\phi_{\text{perfect conductor}}$) is shown by the dashed line in Figure 4, while the solid line depicts the calculated phase (ϕ) of the wave reflected from a dielectric layer placed infront of and in intimate contact ($d_2 = 0$) with the perfect conductor. The normalized phase can then be calculated using Equation 17. The result is shown by the solid line in Figure 5(a), along with experimentally measured values which are shown by the dots. There is excellent agreement between the theory and experiment at frequencies between 4 GHz and 18 GHz, particularly the locations at which the abrupt phase transition (i.e., sudden phase reversal from +180° to –180°) occurs. Some of the sharp features in the calculated phase at frequencies below 9 GHz are not evident in the experimental data. This may be explained by slight variations in the thickness of the rubber layer leading

to the faces of the layer not being perfectly smooth and flat. The theoretically calculated reflectance (Eqn. 16) for these conditions is also in excellent agreement with the measured values between 4 and 17 GHz as shown in Figure 5(b).

The measured phase and reflectance as a function of frequency for the case of a disbond thickness of $d_2 = 1.5$ mm are compared with theory in Figure 6(a) and Figure 6(b) respectively. Again, good agreement is observed between the theory and experiment above 4 GHz.
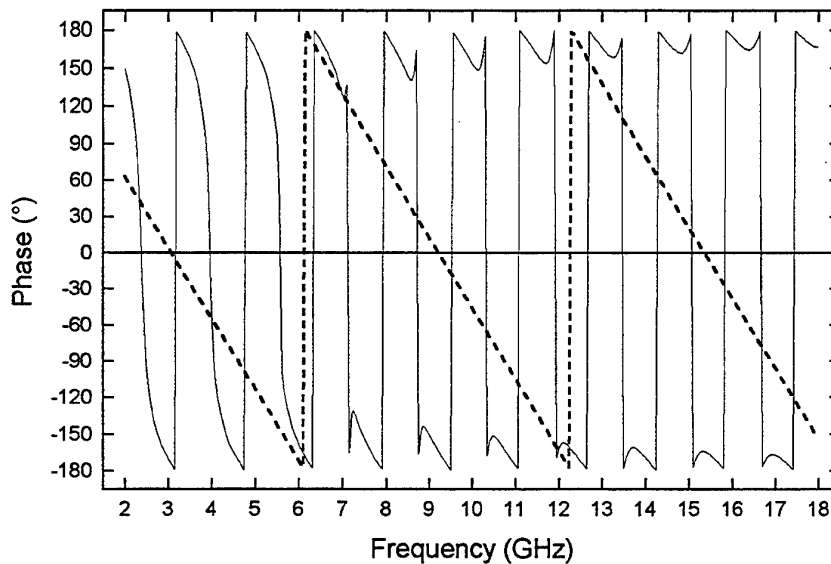

Figure 4: *The theoretically calculated unnormalized phase (solid line) of the reflected wave for the case of no disbond between the isotropic synthetic rubber layer and the perfect conductor backing-plate. The dashed line is the theoretically calculated unnormalized phase of the reflected wave from the perfect conductor backing-plate only.*
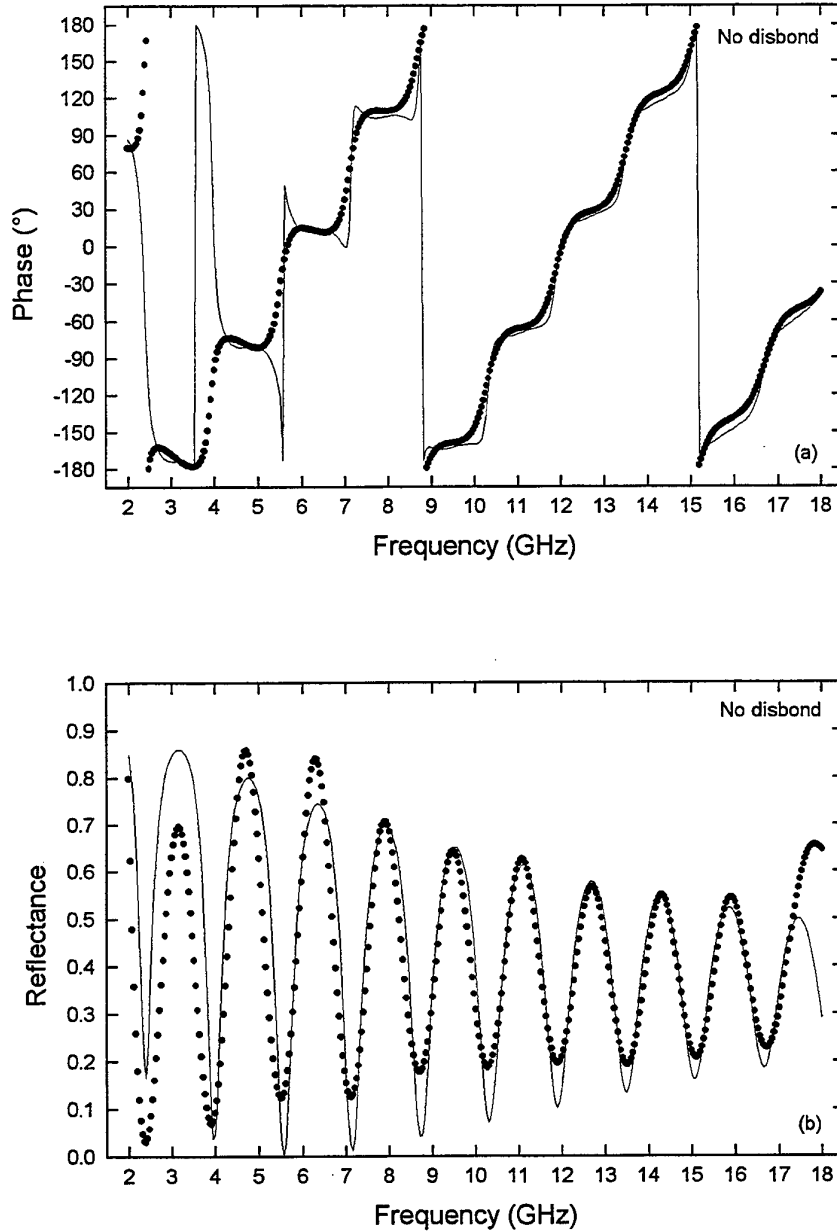
Figure 5: *(a) Phase and (b) reflectance as a function of frequency for the case of no disbond between the isotropic synthetic rubber layer and aluminium backing-plate. The theoretically calculated values are shown by the solid line and the points indicate the measured values.*

Figure 6: *(a) Phase and (b) reflectance as a function of frequency for the case of a 1.5 mm disbond between the isotropic synthetic rubber layer and aluminium backing-plate. The theoretically calculated values are shown by the solid line and the points indicate the measured values.*
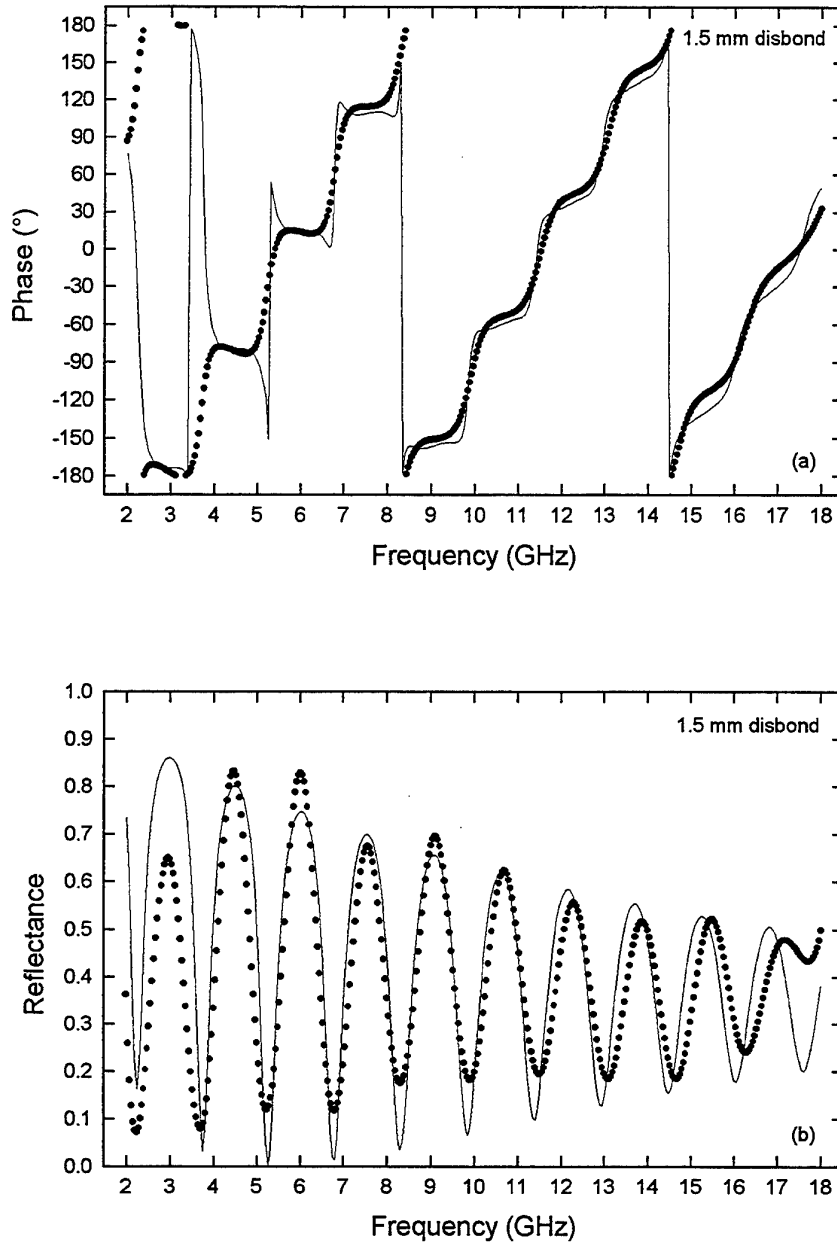
The graphs of reflectance as a function of frequency (Figs. 5(b) and 6(b)) show the familiar oscillatory pattern obtained by the constructive and destructive interference of phase. The thickness of the rubber layer and the real part of the complex relative dielectric constant have a strong influence on the positions of the reflectance peaks, while the imaginary part influences the degree of attenuation and hence the peak heights. The small discrepancy between the positions of calculated and measured reflectance peaks at the higher frequencies shown in Figure 6(b) may be attributed to: a possible slight error in the measurement of the real part of the relative dielectric constant of the rubber layer; possible variations in thickness of the rubber; or variations in the thickness of the disbond provided by the multiple sheets of paper.

Figure 7(a) and 7(b) show the experimental phase and reflectance as a function of frequency respectively, for different disbond thicknesses. It can be clearly seen in Figure 7(a) that as the disbond thickness increases from 0.0 mm to 1.5 mm the location of the phase transition shifts non-uniformly towards lower frequencies. Similarly, the reflectance peaks also shift towards lower frequencies with increasing disbond thickness, as depicted in Figure 7(b).

In Figure 7(a), the phase transitions occur over a range of 0.64 GHz as the disbond thickness is increased from 0 to 1.5 mm. At the next lower phase transition frequency (near 9 GHz in Figure 5(a)), the phase transition occurs over a range of 0.44 GHz. This indicates that the higher transition frequencies are more sensitive to disbond thickness. This is also evident from comparing the positions of the experimental reflectance peaks in Figures 5(b) and 6(b). There is a proportionally greater shift in the peaks at the higher frequencies than at the lower frequencies.

The phase transition frequency as a function of disbond thickness is shown in Figure 8. The measured and calculated values are in good agreement showing a smooth decrease in the transition frequency with increasing disbond thickness.

The frequencies at which the phase is most sensitive to the disbond thickness can be determined by measuring the phase change between the no disbond and disbonded cases. This is calculated by subtracting the phase for the no disbond case from the phase when disbonds are present. This gives the change in phase, $\Delta\phi$, relative to the no disbond case which can be expressed as

$$\Delta\phi = \phi_{disbond} - \phi_{no\ disbond} .$$ (18)

The measured and theoretically calculated change in phase (with respect to the no disbond case) as a function of frequency at different disbond thicknesses are shown in Figures 9(a) and 9(b) respectively. These graphs show that the change in phase ($\Delta\phi$) is strongly frequency dependent. The measured and calculated peak positions are in excellent agreement, while the measured peak heights are smaller than the those calculated, particularly at the lower frequencies. Both figures clearly show a broadening of the peaks with increasing frequency. These peaks correspond to the
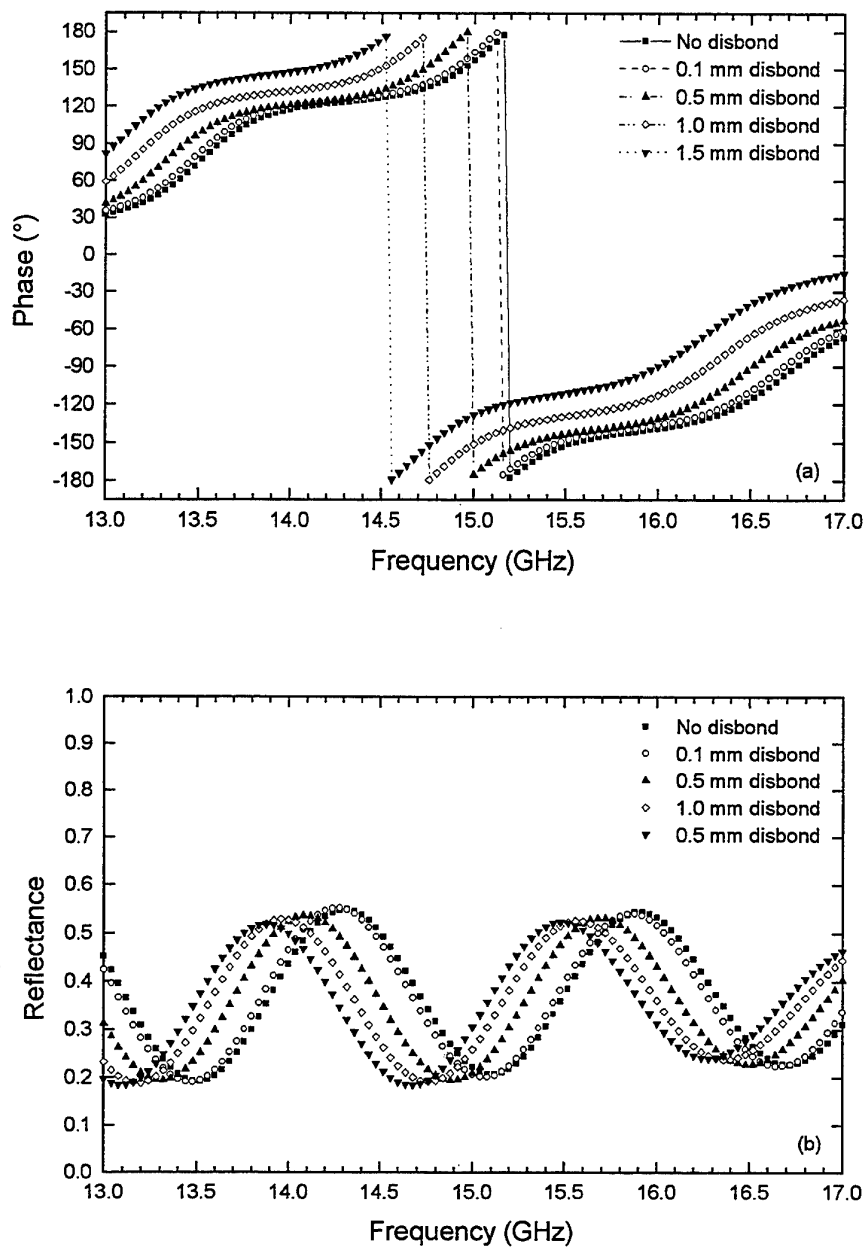
Figure 7: Measured (a) phase and (b) reflectance as a function of frequency for different disbond thicknesses between the isotropic synthetic rubber layer and aluminium backing-plate.

regions where the phase is most sensitive to the disbond thickness for the multi-layer structure considered.

Figure 10 shows the good agreement obtained between the measured and calculated phase as a function of disbond thickness at a single frequency of 13.48 GHz. This frequency corresponds to one of the peaks in Figure 9(a). The steeper initial region of the curve indicates that this method is more sensitive to smaller disbond thicknesses than larger thicknesses.
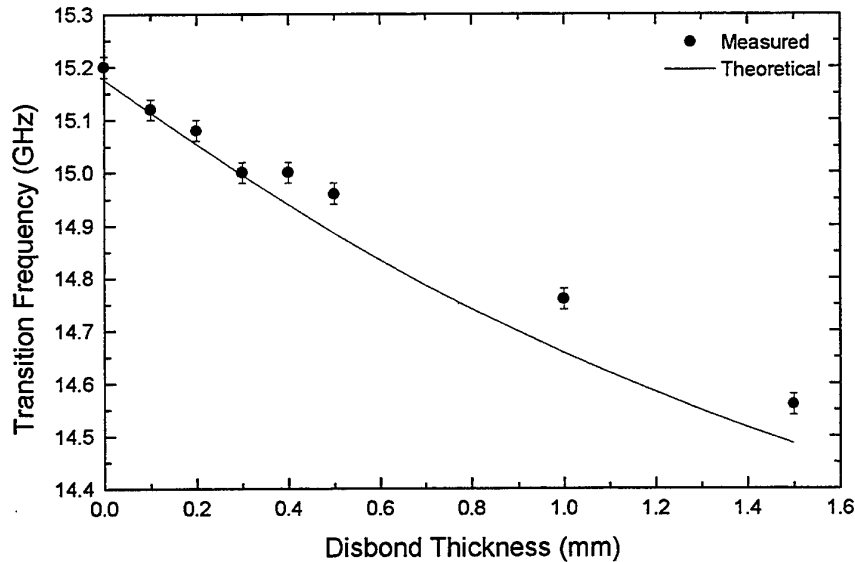

Figure 8: Phase transition frequency (near 15 GHz) as a function of disbond thickness between the isotropic synthetic rubber layer and the conducting-backing plate. The theoretically calculated values are shown by the solid line and the points indicate the measured values.
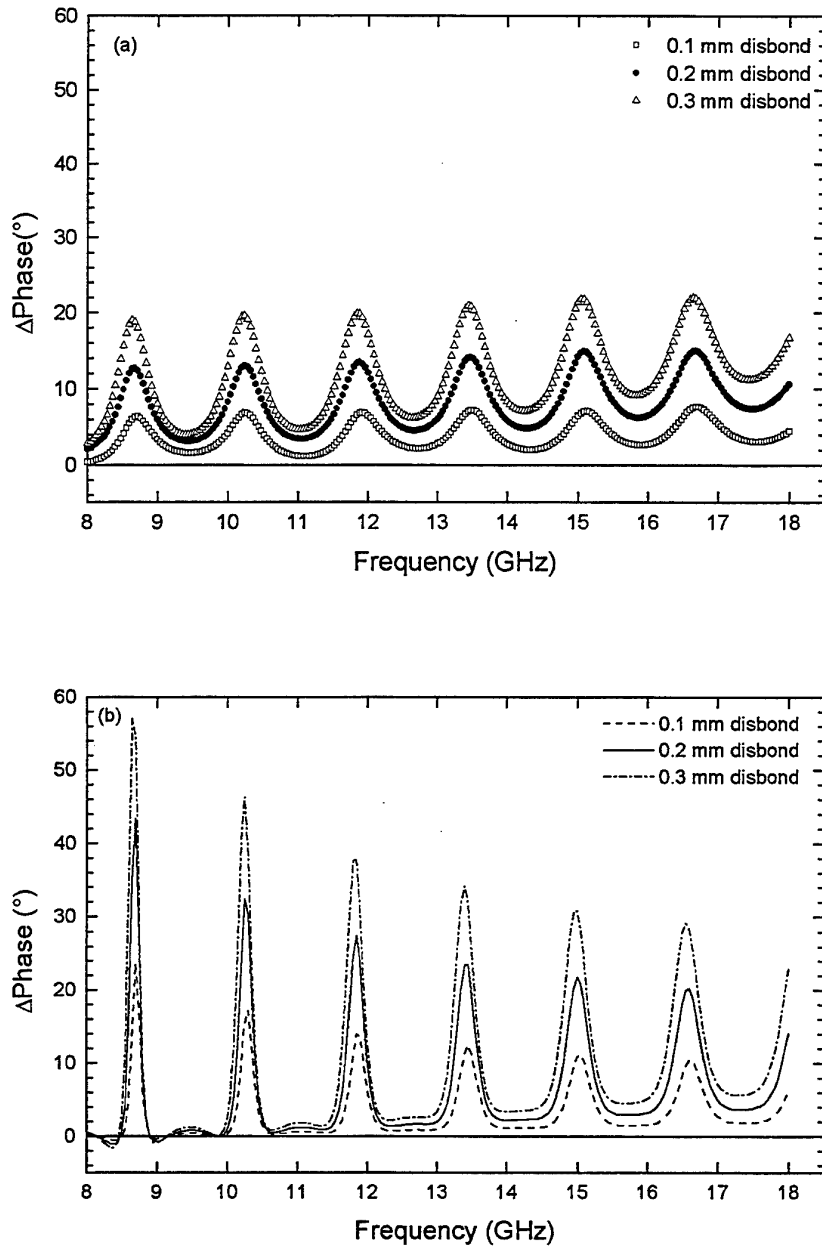
Figure 9: *Change in phase as a function of frequency at disbond thicknesses of 0.1, 0.2 and 0.3 mm between the isotropic synthetic rubber layer and the conducting backing-plate. (a) measured values and (b) theoretically calculated values.*
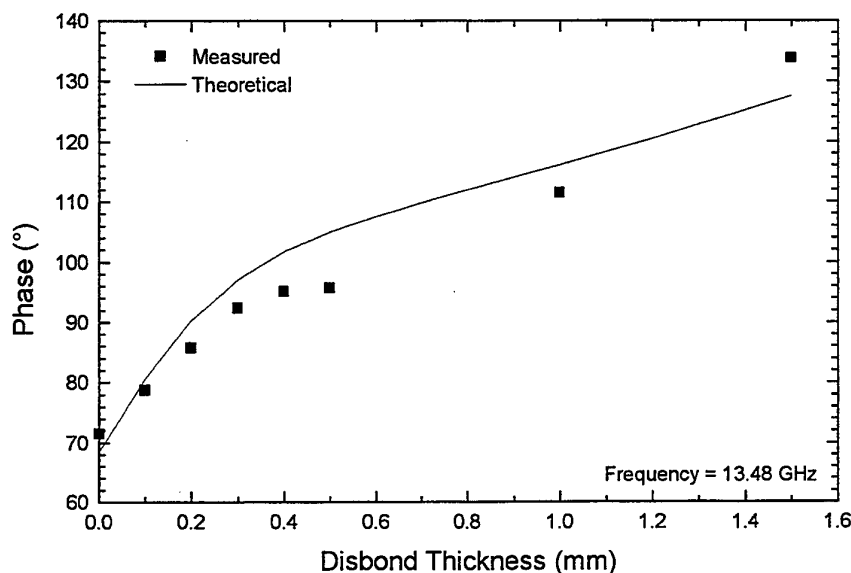
Figure 10: *Phase as a function of disbond thickness between the isotropic synthetic layer and a conducting-backing plate at a frequency of 13.48 GHz. The theoretically calculated values are shown by the solid line and the points indicate the measured values.*

4.2 COLLINS Anechoic Tile

A schematic diagram of a COLLINS anechoic tile is shown in Figure 11. The synthetic rubber tile consists of two regions. The upper region is isotropic and homogeneous while the lower region contains a regular array of hexagonal prism shaped voids of equal size that are open to the surface. For all measurements the lower region was placed facing towards the aluminium backing-plate. The tile has the same relative dielectric permittivity as the rubber layer used in the previous section (i.e., $\varepsilon_1 = 15.0 - j0.7$) and has a thickness of 30.0 mm.

Figure 12 shows the experimental phase as a function of frequency for different disbond thicknesses. Following a trend similar to that shown for the isotropic synthetic rubber layer (Fig. 7(a)), the location of phase transition shifts non-uniformly toward lower frequencies as the disbond thickness increases from 0.0 mm to 1.5 mm. Here the phase transition occurs over a range of 0.60 GHz as the disbond thickness is increased from 0 to 1.5 mm.
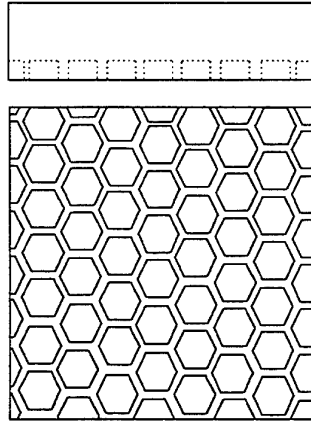
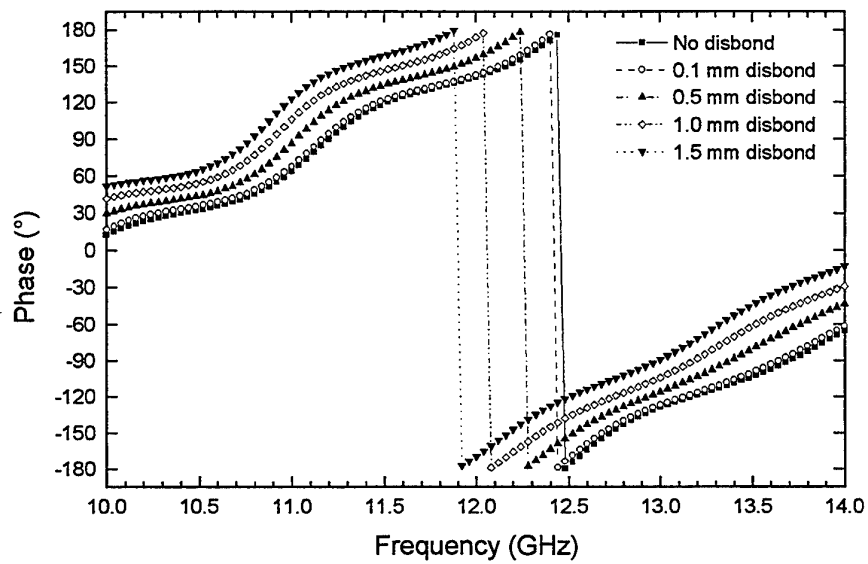Figure 11: *Schematic diagram of an anechoic tile.*

Figure 12: *Measured phase values at different disbond thicknesses between an anechoic tile and an aluminium backing-plate as a function of frequency.*

The phase transition frequency as a function of disbond thickness for the anechoic tile is shown in Figure 13. This graph shows a smooth decrease in the transition frequency with increasing disbond thickness, again a trend similar to that shown in Figure 8.

Figure 14 shows the change in phase as a function of frequency at different disbond thicknesses. As expected from Figures 9(a) and 9(b), the change in phase is frequency dependent, with the peaks corresponding to the frequencies where the phase is most sensitive to the disbond thickness

The measured phase as a function of disbond thickness at a single frequency of 13.76 GHz for the anechoic tile is shown in Figure 15. This frequency corresponds to one of the peaks in Figure 14. The shape of this curve is similar to that shown in Figure 10.
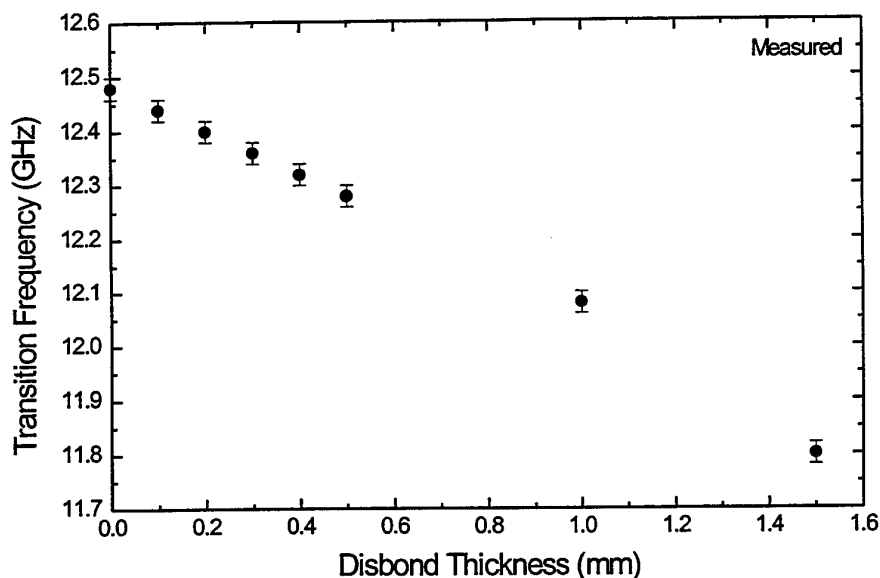
Figure 13: Phase transition frequency as a function of disbond thickness between an anechoic tile and an aluminium backing-plate.

Figure 14: Measured values of change in phase as a function of frequency for disbond thicknesses of 0.1, 0.2 and 0.3 mm between an anechoic tile and an aluminium backing-plate.

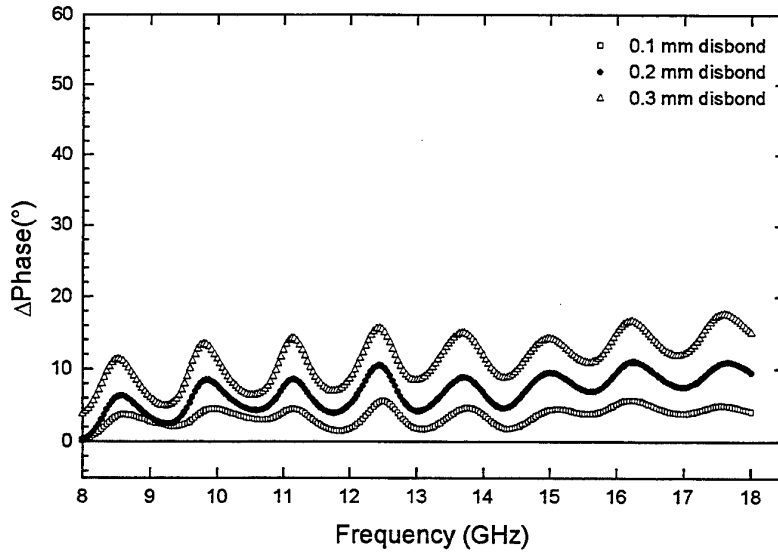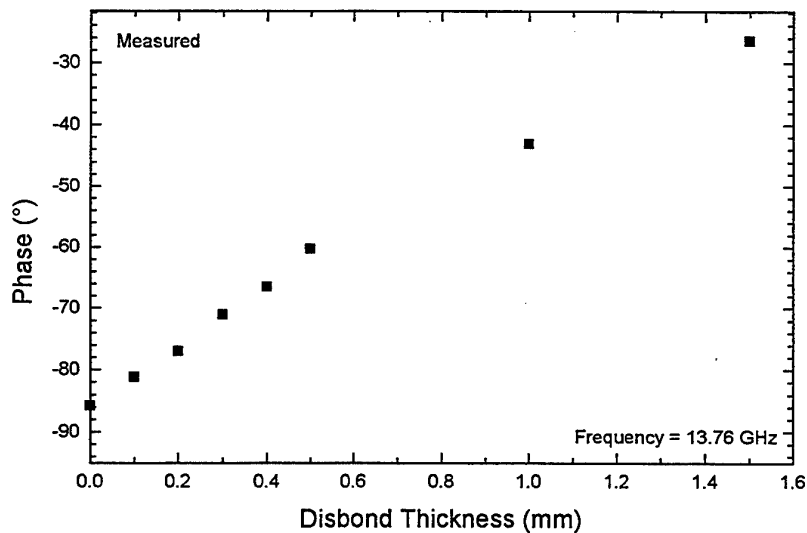*Figure 15: Measured values of phase as a function of disbond thickness between an anechoic tile and an aluminium backing-plate at a frequency of 13.76 GHz.*

5. Discussion

This report has identified two methods utilizing the phase of a reflected microwave signal that are capable of both detecting and quantifying disbonds between a dielectric layer and a conducting backing-plate. The first method involved sweeping the frequency and determining the shift of a phase transition as disbond thickness increased. The second method relied on the difference in phase from a well-bonded case with that of a disbonded case, both measured at a single frequency. From a practical point of view, the second method would be the most appropriate because of the simplicity in choosing a particular frequency and carrying out all measurements at this frequency. The first method would require the frequency to be swept over a range to determine the phase transition frequency.

In practice the single frequency method could be carried out using a comparison technique with the phase of a wave reflected from a well-bonded structure used as a reference. The measured phase would then be subtracted from subsequent phase measurements on regions suspected of containing disbonds. Neglecting any variation in the adhesive thickness or tile thickness, a phase difference will be an indication of the presence of a disbond. Then using a calibration diagram similar to those in Figures 10 and 15 the disbond thickness could be quantified. These figures indicate that the presence of a 0.1 mm (100 μm) disbond can easily be detected and quantified. We have not attempted to evaluate the thickness resolution of this technique, however Edwards and Zoughi [2] show that 10 μm is possible and under favourable conditions 4 μm may be achievable.

Since the phase technique described here is very sensitive to thickness, it would lead to a number of problems in practice. These include non-uniformity in tile thickness, situations where the adhesive may not be applied uniformly and curvature of the backing-plate. However the greatest practical difficulty would be ensuring that the separation between the multi-layer structure being measured and the horn antennae remains constant. Any variation in this separation, for example due to vibration of the structure, will lead to a change in phase which could be misinterpreted as a disbond.

In the present work a disbond with a square shaped area of 150 × 150 mm was investigated. The area resolution of the technique has not been determined and further work is needed to identify the minimum disbond area that is detectable by this method. At frequencies higher than we have considered the horn antenna size is smaller providing increased phase sensitivity and better spatial resolution enabling smaller areas of disbond to be interrogated. However, at such higher frequencies the signal penetration may not be adequate to reach the conducting backing plate and when carrying out the experiments it becomes more important that the tile is replaced in exactly the same position after varying the thickness.

The theoretical model provides important information on the optimization of the measurement frequency to attain the best phase sensitivity to disbonds for the

experimental conditions encountered. The disbond was assumed to have the relative dielectric permittivity of paper. However, in practice a disbond or lack of adhesive will result in thin layer of air separating the dielectric layer and the conducting plate. This case could be modelled just as easily. Also the derivation assumes the flat conducting backing-plate is non-magnetic, and our experimental results were obtained using an aluminium (non-magnetic) plate. At the high frequencies considered our derivation is also valid for the case of a magnetic backing-plate [5]. Therefore, at these frequencies we can treat the ferromagnetic COLLINS-class submarine steel as non-magnetic.

To fully model the COLLINS anechoic tile configuration a 4-layer system would have to be used instead of the 3-layer system presented here. Expressions for a 4-layer system have been derived [3, 4] in a similar manner to those derived here for the 3-layer system. For modelling purposes the anechoic tile could be considered as two discrete layers to account for the hexagonal prism void structure on the underside of the tile. One portion of the tile could be considered isotropic and homogeneous, while the other, as a first approximation, an isotropic inhomogeneous layer composed of spherical voids embedded in a continuous dielectric medium. More elaborate models would include the shape and orientation of the voids (i.e., an anisotropic layer).

We have also performed measurements in the near-field for both an isotropic rubber layer and an anechoic tile placed on a mild steel backing-plate. The experimental results clearly indicate that disbonds can still be detected and quantified in the near-field with a magnetic backing-plate. Since the theory developed here is not valid in the near-field, the thickness of the disbonds can not be determined by this theory but would need be determined experimentally by calibration against known disbond thicknesses.

Further development of this technique is needed before it could be used in practice. Potential problems that need investigating include the effects on the phase due to, the hull curvature, any vibration of the hull and the presence of water under the tile. Because of the inability to use this technique underwater an approach using ultrasonics is currently being investigated which is more promising for immediate in-situ application.

6. Conclusion

A simple non-contact nondestructive technique capable of both detecting and quantifying the thickness of a disbond between a low-loss dielectric layer and a conducting plate has been presented. The technique relies on the measurement of the phase of the amplitude reflection coefficient for plane-wave microwave radiation incident on the structure.

A theoretical model for predicting the magnitude and phase of a reflected microwave signal in the absence and presence of a disbond has been derived. The theoretical phase calculations as a function of frequency and disbond thickness were compared with experiment with excellent agreement. The experimental results clearly indicate that a disbond of 0.1 mm between the dielectric layer and the conducting plate can easily be resolved under laboratory conditions. Further refinements are required before this technique can be implemented as a practical and reliable method for detecting disbonds under COLLINS anechoic tiles in field conditions.

7. Acknowledgements

8. References

1 Zoughi, R. and Lujan, M. (1989) Nondestructive microwave thickness measurements in dielectric slabs, *Mater. Eval.* **48** (1100–1105)

2 Edwards, J. and Zoughi, R. (1993) Microwave sensitivity maximization of disbond characterization in conductor backed dielectric composites, *J. Nondestr. Eval.* **12** (193–198)

3 Zoughi, R. and Bakhtiari, S. (1990) Microwave nondestructive detection and evaluation of disbonding and delamination in layered-dielectric-slabs, *IEEE Trans. Instr. Meas.* **39** (1059–1063)

4 Zoughi, R., Edwards, J. and Bakhtiari, S. (1992) Swept microwave frequency nondestructive detection and evaluation of delamination in stratified dielectric media, *J. Wave-Mater. Interact.* **7** (1–12)

5 Borzorth, R.M., *Ferromagnetism*, (D. Van Nostrand, New York, 1953)

DISTRIBUTION LIST

Microwave Nondestructive Evaluation of Disbonds Under Anechoic Tiles

R.J. Ditchburn, A. Amiet and S.K. Burke

1. DEFENCE ORGANISATION

a. Task sponsor   DNER-SM

b. S&T Program
Chief Defence Scientist
FAS Science Policy   } shared copy
AS Science Industry and External Relations
AS Science Corporate Management
Counsellor Defence Science, London (Doc Data Sheet)
Counsellor Defence Science, Washington (Doc Data Sheet)
Scientific Adviser to Thailand MRDC (Doc Data Sheet)
Senior Defence Scientific Adviser/Scientific Adviser Policy and Command
        (shared copy)
Navy Scientific Adviser
Scientific Adviser - Army (Doc Data Sheet and distribution list only)
Air Force Scientific Adviser
Director Trials

Aeronautical and Maritime Research Laboratory
Director
Chief, SSMD
D. Bradhurst
B. Dixon
R.J. Ditchburn
A. Amiet
S.K. Burke
D. Oldfield

Electronics and Surveillance Research Laboratory
Director

DSTO Library
Library Fishermens Bend
Library Maribyrnong
Library DSTOS (2 copies)
Library, MOD, Pyrmont (Doc Data sheet only)
Australian Archives

c. Forces Executive
Director General Force Development (Sea)
Director General Force Development (Land) (Doc Data Sheet only)
Director General Force Development (Air) (Doc Data Sheet only)

d. Navy
SO (Science), Director of Naval Warfare, Maritime Headquarters Annex, Garden
        Island, NSW 2000 (Doc Data Sheet only)

e. Army
ABCA Office, G-1-34, Russell Offices, Canberra   (4 copies)

f. Air Force
No compulsory distribution

g. S&I Program
Defence Intelligence Organisation
Library, Defence Signals Directorate (Doc Data Sheet only)

h. Acquisition and Logistics Program
No compulsory distribution

i. B&M Program (libraries)
OIC TRS, Defence Central Library
Officer in Charge, Document Exchange Centre (DEC), 1 copy
        DEC requires the following copies of public release reports to meet
           exchange agreements under their management:
        *US Defence Technical Information Centre, 2 copies
        *UK Defence Research Information Centre, 2 copies
        *Canada Defence Scientific Information Service, 1 copy
        *NZ Defence Information Centre, 1 copy
        National Library of Australia, 1 copy

2. UNIVERSITIES AND COLLEGES

Australian Defence Force Academy
    Library
    Head of Aerospace and Mechanical Engineering
Deakin University, Serials Section (M list), Deakin University Library, Geelong, 3217
Senior Librarian, Hargrave Library, Monash University
Librarian, Flinders University

3. OTHER ORGANISATIONS

NASA (Canberra)
AGPS

OUTSIDE AUSTRALIA

4. ABSTRACTING AND INFORMATION ORGANISATIONS
    INSPEC: Acquisitions Section Institution of Electrical Engineers
    Library, Chemical Abstracts Reference Service
    Engineering Societies Library, US
    American Society for Metals
    Documents Librarian, The Center for Research Libraries, US

5. INFORMATION EXCHANGE AGREEMENT PARTNERS
    Acquisitions Unit, Science Reference and Information Service, UK
    Library - Exchange Desk, National Institute of Standards and Technology,
US

SPARES (10 copies)

Total number of copies: 57

DEFENCE SCIENCE AND TECHNOLOGY ORGANISATION DOCUMENT CONTROL DATA			1. PRIVACY MARKING/CAVEAT (OF DOCUMENT)		
2. TITLE Microwave Nondestructive Evaluation of Disbonds Under Anechoic Tiles			3. SECURITY CLASSIFICATION (FOR UNCLASSIFIED REPORTS THAT ARE LIMITED RELEASE USE (L) NEXT TO DOCUMENT CLASSIFICATION) Document (U) Title (U) Abstract (U)		
4. AUTHOR(S) R.J. Ditchburn, A.Amiet and S.K. Burke			5. CORPORATE AUTHOR Aeronautical and Maritime Research Laboratory PO Box 4331 Melbourne Vic 3001		
6a. DSTO NUMBER DSTO-TR-0398	6b. AR NUMBER AR-009-804		6c. TYPE OF REPORT Technical Report	7. DOCUMENT DATE July 1996	
8. FILE NUMBER M1/8/896	9. TASK NUMBER 95/071	10. TASK SPONSOR DNER-SM	11. NO. OF PAGES 25	12. NO. OF REFERENCES 5	
13. DOWNGRADING/DELIMITING INSTRUCTIONS None			14. RELEASE AUTHORITY Chief, Ship Structures and Materials Division		

15. SECONDARY RELEASE STATEMENT OF THIS DOCUMENT

Approved for public release

OVERSEAS ENQUIRIES OUTSIDE STATED LIMITATIONS SHOULD BE REFERRED THROUGH DOCUMENT EXCHANGE CENTRE, DIS NETWORK OFFICE, DEPT OF DEFENCE, CAMPBELL PARK OFFICES, CANBERRA ACT 2600

16. DELIBERATE ANNOUNCEMENT

No limitations

17. CASUAL ANNOUNCEMENT	Yes

18. DEFTEST DESCRIPTORS

Microwaves; Nondestructive Inspection; Collins class submarines; Bonding

19. ABSTRACT
An experimental and theoretical study of a microwave nondestructive inspection technique to detect the presence of and evaluate the thickness of disbonds between anechoic tiles and the hull of the COLLINS-class submarine is presented. The magnitude and phase of a reflected microwave signal in the absence and presence of a disbond is measured as a function of disbond thickness and frequency for (i) a layer of anechoic tile material and (ii) a COLLINS anechoic tile, both backed by a flat conducting plate. Disbond thicknesses of 0.0 to 1.5 mm are considered over a frequency range of 2 to 18 GHz. The results are in good agreement with theoretical predictions and clearly indicate that disbonds of 0.1 mm can be easily detected. Further development and potential problems are also described.